Received: 3 April 2018 | Accepted: 20 June 2018

DOI: 10.1111/cas.13710

ORIGINAL ARTICLE

WILEY Cancer Science

EWS-FLI1 regulates a transcriptional program in cooperation with Foxq1 in mouse Ewing sarcoma

Rikuka Shimizu[1,2] | Miwa Tanaka[1] | Shuichi Tsutsumi[3] | Hiroyuki Aburatani[3] | Yukari Yamazaki[1] | Mizuki Homme[1] | Yoshimasa Kitagawa[2] | Takuro Nakamura[1]

[1]Division of Carcinogenesis, The Cancer Institute, Japanese Foundation for Cancer Research, Tokyo, Japan

[2]Department of Oral Diagnosis and Medicine, Faculty of Dental Medicine, Hokkaido University, Sapporo, Japan

[3]Genome Science Division, Research Center for Advanced Science and Technology, The University of Tokyo, Tokyo, Japan

Correspondence: Takuro Nakamura, Division of Carcinogenesis, The Cancer Institute, Japanese Foundation for Cancer Research, Tokyo, Japan (takuro-ind@umin.net).

Funding information
Mitsubishi Foundation, Grant/Award Number: 29133; Japan Society for the Promotion of Science, Grant/Award Number: 16K07131, 26250029

EWS-FLI1 constitutes an oncogenic transcription factor that plays key roles in Ewing sarcoma development and maintenance. We have recently succeeded in generating an ex vivo mouse model for Ewing sarcoma by introducing EWS-FLI1 into embryonic osteochondrogenic progenitors. The model well recapitulates the biological characteristics, small round cell morphology, and gene expression profiles of human Ewing sarcoma. Here, we clarified the global DNA binding properties of EWS-FLI1 in mouse Ewing sarcoma. GGAA microsatellites were found to serve as binding sites of EWS-FLI1 albeit with less frequency than that in human Ewing sarcoma; moreover, genomic distribution was not conserved between human and mouse. Nevertheless, EWS-FLI1 binding sites within GGAA microsatellites were frequently associated with the histone H3K27Ac enhancer mark, suggesting that EWS-FLI1 could affect global gene expression by binding its target sites. In particular, the Fox transcription factor binding motif was frequently observed within EWS-FLI1 peaks and Foxq1 was identified as the cooperative partner that interacts with the EWS portion of EWS-FLI1. *Trib1* and *Nrg1* were demonstrated as target genes that are co-regulated by EWS-FLI1 and Foxq1, and are important for cell proliferation and survival of Ewing sarcoma. Collectively, our findings present novel aspects of EWS-FLI1 function as well as the importance of GGAA microsatellites.

KEYWORDS
Ewing sarcoma, EWS-FLI1, Foxq1, GGAA microsatellite, Trib1

1 | INTRODUCTION

Ewing sarcoma is a highly malignant bone tumor affecting children and adolescents.[1] Chromosome translocations involving 22q12 generate EWS-ETS fusion proteins; of these, EWS-FLI1 is the most frequently detected fusion, which is causally associated with Ewing sarcoma and plays a crucial role in carcinogenesis, tumor cell maintenance, and disease progression.[2-5] Transcriptional regulation of downstream target genes by EWS-FLI1 determines the phenotypes of Ewing sarcoma and affects sensitivity to therapies. A specific epigenetic status is important for the oncogenic action of EWS-FLI1.[5-7] Moreover, EWS-FLI1 actively modulates overall epigenetic conditions by binding *cis* elements in the genome.[4,8]

We have established an ex vivo mouse model for Ewing sarcoma by introducing EWS-FLI1 cDNA into embryonic osteochondrogenic progenitor cells.[5] The model well recapitulates the morphologies and gene expression profiles of human Ewing sarcoma. In addition, murine Ewing sarcoma is highly dependent on

Abbreviations: ChIP-Seq, chromatin immunoprecipitation and sequencing; EMT, epithelial-mesenchymal transition; eSZ, embryonic superficial zone; ES, Ewing sarcoma; FC, fold change; FoBS, Fox binding site; GEO, Gene Expression Omnibus; H3K27Ac, H3 lysine 27 acetylation; H3K27me3, H3 lysine 27 trimethylation; TSS, transcription start site.

EWS-FLI1 expression, indicating that EWS-FLI1 drives the expression of genes important for cell survival and proliferation. Thus, it is worthwhile to clarify whether EWS-FLI1 binds DNA and remodels chromatin in mouse sarcoma cells similar to human Ewing sarcoma. Given that the mutation rate is quite low and few recurrent mutations occur in human Ewing sarcoma,[9-11] EWS-FLI1 and its interaction with the appropriate epigenetic condition are considered to be responsible for the core biological functions of Ewing sarcoma.

Previous studies showed that EWS-FLI1 binds to both canonical Ets binding sites and GGAA microsatellites to regulate downstream target genes.[4,12,13] Notably, GGAA microsatellite-associated EWS-FLI1-binding sites are frequently linked to active enhancers and show drastic transactivation by EWS-FLI1, thus emphasizing the significance of these microsatellites. However, the distribution of GGAA microsatellites is not well conserved between human and mouse.[12] Despite this difference, the gene expression profile of Ewing sarcoma in mouse resembles that of human,[5] indicating the importance of clarifying EWS-FLI1 binding in the mouse Ewing sarcoma model. Moreover, EWS-FLI1–dependent survival and proliferation of mouse Ewing sarcoma strongly suggests the common important function of EWS-FLI1 among different organisms. It is therefore important to clarify global EWS-FLI1 binding in mouse Ewing sarcoma and to evaluate the difference and similarity with that in the human counterpart.

Here, we identified global DNA binding of EWS-FLI1 in mouse Ewing sarcoma. EWS-FLI1 recognizes GGAA microsatellites, although the frequency is much less than that in human Ewing sarcoma. Moreover, the genes nearest the binding sites in mouse differ considerably from those in humans, suggesting that chromatin remodeling by EWS-FLI1 at the higher order topology might play a crucial role in Ewing sarcoma development and maintenance. We have also identified Foxq1 as a novel cooperative transcription factor that interacts with EWS-FLI1. These results show novel functional aspects of EWS-FLI1 in Ewing sarcoma development.

2 | MATERIALS AND METHODS

2.1 | Cell culture and human sarcoma specimens

Mouse Ewing sarcoma cell lines ES48 and ES49 derived from the mouse Ewing sarcoma model were cultured in Iscove's modified Dulbecco's medium supplemented with 10% FBS. Human Ewing sarcoma cell lines EWS and KH established from Ewing sarcoma patient samples[5] were cultured in RPMI-1640 medium supplemented with 10% FBS and 1% HEPES. 293T, U937, KAS, and U2OS were incubated in DMEM supplemented with 10% FBS, 1% HEPES, and 1% nonessential amino acids. Ewing sarcoma, rhabdomyosarcoma, synovial sarcoma, and osteosarcoma samples were obtained from the Cancer Institute Hospital. Informed consent was obtained from the donors, and the study was approved by the Institutional Review Board at the Japanese Foundation for Cancer Research under license 2013-1155.

2.2 | Chromatin immunoprecipitation and sequencing

Chromatin immunoprecipitation and sequencing was carried out using the method previously described with modifications.[14] A total of 5×10^7 cells per immunoprecipitation were fixed with 1% formaldehyde for 10 minutes at 37°C. Chromatin was sheared in SDS lysis buffer containing 1% SDS, 10 mmol/L EDTA, and 50 mmol/L Tris pH 8.0 to an average size of 400 to 500 bp using a Covaris S220 sonicator (Covaris, Woburn, MA, USA) for 5 minutes. ChIP was carried out with 4 μg anti-histone H3K27Me3 (Abcam, Cambridge, UK), anti-histone H3K27Ac (Active Motif, Carlsbad, CA, USA), or anti-FLAG M2 (Sigma, St Louis, MO, USA) antibodies. The antibody-bound protein/DNA complexes were immunoprecipitated using protein G magnetic beads. Immunoprecipitated DNA was then purified and subjected to secondary sonication to an average size of 150 to 350 bp. Libraries were prepared according to instructions accompanying the ThruPLEX DNA-Seq kit (Rubicon Genomics, Ann Arbor, MI, USA). The ChIP DNA was end modified, and adapters were ligated. DNA was PCR amplified with Illumina primers, and Illumina-compatible indexes were added (San Diego, CA, USA). Library fragments of approximately 300-500 bp were band-isolated from an agarose gel. The purified DNA was sequenced on an Illumina MiSeq next-generation sequencer following the manufacturer protocols. Base calls were carried out using Bowtie 1.1.1 (http://bowtie-bio.sourceforge.net/index.shtml). ChIP-Seq reads were aligned to the mm9 genome assembly (https://www.ncbi.nlm.nih.gov/grc/mouse) using Samtools 1.2 (http://www.htslib.org). Peak calling was carried out using MACS1.4 (http://liulab.dfci.harvard.edu/MACS). Peak distribution was calculated by PEAKS v1.2 (http://133.130.70.33/PEAKSv1.2_beta). Neighbor genes on enriched genomic regions were determined using Cell Innovation Program (https://cell-innovation.nig.ac.jp). Results were visualized using IGV_2.3.80 (http://software.broadinstitute.org/software/igv). EWS-FLI1-binding motifs were searched using the AME (MEME-Suit Version 4.12.0) program (http://meme-suite.org/index.html). Super-enhancers were identified using the method previously described[15,16] with the ROSE program (http://younglab.wi.mit.edu/super_enhancer_code.html).

2.3 | Microarray analysis

GeneChip analysis was conducted to determine gene expression profiles. Total RNA was extracted using the RNeasy Mini Kit (Qiagen, Venlo, the Netherlands). The murine Genome HT MG-430 PM Array (Affymetrix, Santa Clara, CA, USA) was hybridized with aRNA probes generated from mouse Ewing sarcoma tissue. After staining with streptavidin-phycoerythrin conjugates, arrays were scanned using an Affymetrix GeneAtlas Scanner and analyzed using GeneSpring GX 12.6 (Agilent Technologies, Santa Clara, CA, USA).

2.4 | Real-time quantitative PCR

Total RNA was extracted using the RNeasy Plus Mini Kit (Qiagen) according to manufacturer's protocol. cDNA was synthesized from 1 μg total RNA using a reverse transcription system (Promega, Fitchburg, WI, USA). Real-time quantitative PCR (RT-qPCR) was carried out using Power SYBR Green (Thermo Fisher Scientific, Waltham, MA, USA). The primers used are listed in Table S1.

2.5 | RNA interference studies

siRNAs for knockdown of *FLI1*, *Foxb1*, *Foxq1/FOXQ1*, *Trib1/TRIB1*, and *Nrg1/NRG1* were purchased from Qiagen and Dharmacon (Lafayette, CO, USA) and introduced into mouse or human Ewing sarcoma cells according to manufacturer's protocol. Knockdown efficiencies were confirmed by western blotting using rabbit anti-FOXQ1 antibody (Aviva Systems Biology, San Diego, CA, USA), mouse monoclonal anti-HA (MBL, Nagoya, Japan), or rabbit anti-FLI1 (Abcam) antibodies, or qPCR. The list of siRNAs is shown in Table S2.

2.6 | Luciferase assay

Genomic DNA fragments containing both GGAA microsatellites and Fox binding motifs of *Trib1* and *Nrg1* were cloned into a pGL3 promoter vector (Promega). FLAG-tagged *EWS-FLI1* and HA-tagged *Foxq1* cDNAs were cloned into pMSV or pcDNA3.1, respectively. Inserts were generated by PCR with appropriate primers (Table S1). A total of 1×10^5 U2OS cells were transfected with the above-mentioned plasmids in indicated combinations. Cells were harvested 48 hours after transfection, and luciferase assays were carried out using the Dual-reporter Luciferase Assay System (Promega) according to manufacturer's procedure.

2.7 | Co-immunoprecipitation assays

ES49 cells were transfected with pcDNA HA-Foxq1, and 293T cells were co-transfected with HA-tagged Foxq1 and FLAG-tagged EWS-FLI1. Cells were lysed 48 hours after transfection in RIPA buffer and incubated with mouse monoclonal anti-HA, anti-FLAG (Sigma), or control IgG for 1 hour at 4°C and immunoprecipitated with Protein A Agarose beads (GE Healthcare, Chicago, IL, USA) for 1 hour at 4°C. After washing 3 times, the precipitated proteins were eluted by boiling in Laemmli sample buffer. Proteins were separated by SDS-PAGE, blotted onto nitrocellulose membranes, and incubated with the indicated primary antibodies.

2.8 | Cell proliferation, apoptosis, and cell cycle assays

A total of 5×10^4 ES49 cells or 1×10^5 EWS cells were seeded in 12-well plates. HA-tagged Trib1 and Nrg1 cDNAs were subcloned into pCDNA3.1 and transfected into ES49 or EWS cells. Cell proliferation was determined by measuring cell numbers 48 and/or 72 hours after siRNA treatment using the Countess cell number counter (Invitrogen, La Jolla, CA, USA). For apoptosis and cell cycle assays, siRNA-treated cells were cultured with an FBS-depleted medium (0.5% FBS) for 48 hours. To detect apoptotic cells, cells were stained for Annexin-V using an FITC-conjugated Annexin-V antibody (BD Biosciences, Franklin Lakes, NJ, USA). DNA synthesis was assessed by 5-ethynyl-2′-deoxyuridine (EdU) incorporation using the Click-iT EdU Alexa Fluor 647 detection kit (Molecular Probes, Eugene, OR, USA). Processed cells were examined by FACSCalibur Flow Cytometer (BD Biosciences). FOXQ1 was detected by immunoblotting.

2.9 | Human microarray analysis

The mRNA expression levels of *FOXQ1*, *FOXF1*, *FOXB1*, *TRIB1*, and *NRG1* in samples from patients with sarcoma were examined by expression profiling by microarray (HG-U133_Plus_2) on the NCBI GEO database (http://www.ncbi.nlm.nih.gov/geo). Ewing sarcoma: GSE12102, alveolar soft part sarcoma: GSE32569, osteosarcoma: GSE87437, rhabdomyosarcoma: GSE66533, and synovial sarcoma: GSE20196 were assessed using GeneSpring GX 12.6.

2.10 | Accession number

The ChIP-Seq data sets are accessible through the NCBI GEO database (http://www.ncbi.nlm.nih.gov/geo), with accession number GSE108631, and the microarray data sets with GSE86502 and GSE90978.

2.11 | Statistical analysis

Statistical significances were compared with a 2-tailed Student's *t* test for comparison between 2 groups to determine the *P*-values and significance shown in the figures and legends.

3 | RESULTS

3.1 | EWS-FLI1 binds enhancer elements in mouse Ewing sarcoma cells

To identify EWS-FLI1-binding sites, we used mouse Ewing sarcoma cell lines ES48 and ES49, which were established from the ex vivo Ewing sarcoma model[5] induced by retroviral introduction of FLAG-tagged human *EWS-FLI1* cDNA (Figure 1A). ChIP-Seq was carried out using an anti-FLAG antibody. A total of 576 EWS-FLI1-binding peaks were detected in ES49 (Doc. S1). The peaks were distributed in promoter, intergenic, and intragenic regions at frequencies of 0.34%, 20.8%, and 78.8%, respectively (Figure 1B). The distribution pattern is comparable to that in human Ewing sarcoma.[4] To show the epigenetic environment around the EWS-FLI1-binding regions, histone modifications including histone H3 lysine 27 acetylation (H3K27Ac) and H3 lysine 27 trimethylation (H3K27me3) were also mapped (Doc.

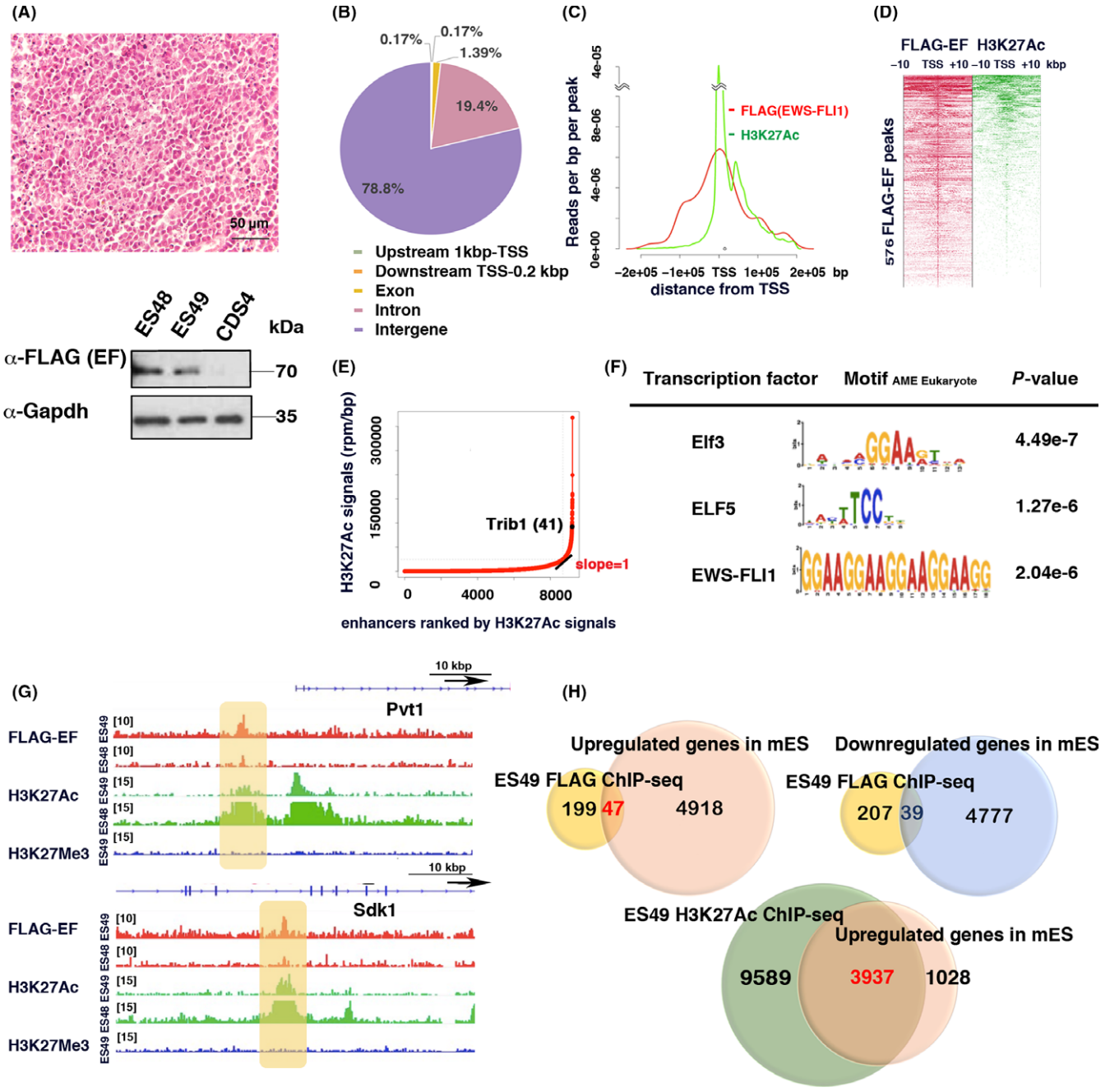

FIGURE 1 Global EWS-FLI1 binding in mouse Ewing sarcoma. A, Histology of mouse Ewing sarcoma, ES49, used for ChIP-Seq analysis. Hematoxylin and eosin staining (top). FLAG-tagged EWS-FLI1 expression was detected by western blotting. CIC-DUX4 sarcoma (CDS4)[17] was used as a negative control (bottom). B, Global distribution of EWS-FLI1-binding sites in relation to known genes. C, Distribution of EWS-FLI1-binding peaks and histone H3K27Ac peaks in relation to transcriptional start sites (TSS) of known genes. D, Density plots of signal intensities of EWS-FLI1 and H3K27Ac peaks from TSS. E, Total H3K27Ac ChIP-Seq signal in units of reads per million in enhancer regions for all enhancers in the ES49 cell line. Enhancers are ranked by increasing H3K27Ac ChIP-Seq signal. F, AME suite motif analysis carried out on EWS-FLI1 binding sites. Ets binding motifs (Elf3 and ELF5) and GGAA microsatellites (EWS-FLI1) were efficiently detected. G, EWS-FLI1 binds to GGAA microsatellites at *Pvt1* and *Sdk1* loci. H3K27Ac signals accompanying these binding sites are highlighted in yellow. Arrows indicate the transcriptional orientation of each gene. H, Venn diagrams for EWS-FLI1 (FLAG) and H3K27Ac ChIP-Seq signals and up- or downregulated genes depicted by microarray analysis

S1). Of the total EWS-FLI1-binding peaks, 21.3% overlapped with H3K27Ac peaks (Table 1), suggesting that EWS-FLI1 is frequently associated with promoter regions as well as with distal enhancer elements, as with human Ewing sarcoma.[18] In particular, EWS-FLI1-binding sites were frequently associated with H3K27Ac peaks on enhancer elements and TSS (Figure 1C,D). In addition, 3% of EWS-FLI1-binding peaks were located in 527 super-enhancer sites showing dense accumulation of H3K27Ac (Figure 1E). *Trib1* constitutes 1 such gene, showing EWS-FLI1 binding at the super-enhancer (see below).

TABLE 1 EWS-FLI1-binding peaks in mouse Ewing sarcoma

Peaks	GGAA microsatellites (+)	GGAA microsatellites (−)
Total peaks (576)	60	516
Peaks overlapped with H3K27Ac	53	70
Peaks overlapped with H3K27Me3	1	119
Peaks overlapped with H3K27Ac and H3K27Me3	0	33
Peaks at super-enhancer	15	1

Motif analysis indicated that Ets-binding sites (EBS) and GGAA microsatellites were significantly enriched within the EWS-FLI1-binding regions as reported in human Ewing sarcoma, albeit with decreased frequency (Figure 1F,G).[4,12,13] H3K27Ac peaks were detected in 88% of EWS-FLI1-binding peaks associated with GGAA microsatellites (Table 1), indicating that the EWS-FLI1 associated with GGAA microsatellites is likely involved in the chromatin remodeling machinery. Moreover, 25% of GGAA microsatellite-associated peaks were defined as super-enhancers. In contrast, no significant association was observed between H3K27me3 peaks and EWS-FLI1-binding peaks on GGAA microsatellites (Table 1). When we compared 246 genes located near EWS-FLI1-binding sites with the genes showing altered expression as detected by microarray analyses of mouse Ewing sarcoma tissue (Doc. S2), 47 upregulated genes and 39 downregulated genes were assigned as nearest neighbor genes for EWS-FLI1-binding peaks (FC >1.5, $P < .05$) (Figure 1H; Doc. S3). Among the upregulated genes, 26 (55.3%) were associated with GGAA microsatellites of which all were accompanied by H3K27Ac-binding peaks. These genes, including *Nrg1*, *Pvt1*, *Rap2b*, *Trib1*, *Mapkap1*, and *Ptprd*, are thus considered as candidate target genes of EWS-FLI1 (Table 2). In human Ewing sarcoma, a number of EWS-FLI1 target genes such as *IGF1*, *NKX2-2*, *NR0B1*, *EZH2*, and *PDGFR* have been reported.[20,21] However, the majority of human Ewing sarcoma candidate target genes were not identified as nearest genes of EWS-FLI1-binding sites in mouse Ewing sarcoma. Overall, only 21 genes were identified in both ES49 and SKNMC human Ewing sarcoma cells (Doc. S4), in which 1314 genes showing EWS-FLI1 binding were reported by Riggi et al.[4]

3.2 | Co-segregation of DNA binding between EWS-FLI1 and FOX transcription factors in Ewing sarcoma

Motif analysis for EWS-FLI1-binding sites showed enrichment for the binding motif of FOX family transcription factors (Figure 2A). This result suggests that multiple genes might be co-regulated by EWS-FLI1 and FOX family transcription factors. A microarray analysis of mouse Ewing sarcoma tissues showed that *Foxd4*, *Foxg1*, *Foxq1*, *Foxf1a*, *Foxf2*, and *Foxb1* were highly expressed among 44 Fox family genes (Figure 2B). The normalized intensity values of

TABLE 2 Candidate targets of EWS-FLI1 associated with GGAA microsatellites within EWS-FLI1-binding peaks

Gene ID	Fold change[a]	FoBS from GGAA[b]
Zfp804a	25.58	46
Cacna2d1	18.23	12
Nrg1	17.91	38
Mmel1	17.17	NI
Rtn4rl1	12.68	NI
Tmtc2	10.29	39
Fam198b	8.82	51
Pvt1	8.08	68
BC030870	7.44	80
Dner	6.85	NI
Herc3	5.28	18
Rap2b	4.52	79
Dync2h1	3.60	100
Trib1	3.51	8
Rpe	3.01	31
Stk3	2.03	NI
Tpcn1	1.95	NI
Agpat9	1.92	0
Fgf12	1.89	28
Cdh23	1.72	NI
Ccdc57	1.70	93
Mapkap1	1.68	27
Ptprd	1.63	0
Rapgef4	1.60	47
Foxk1	1.56	48
Dhx35	1.50	51

[a]Fold change of expression in mouse Ewing sarcoma against a mixture of mouse normal tissues.[19]

[b]Distance (bp) between Fox binding sites (FoBS) and GGAA microsatellites within EWS-FLI1-binding peaks. NI, FoBS not included.

Foxd4, *Foxg1*, *Foxq1*, *Foxf1a*, *Foxf2*, and *Foxb1* in Ewing sarcoma compared with eSZ, in which the cell-of-origin of Ewing sarcoma is enriched,[5] were 162, 46.6, 13.9, 12.0, 8.8, and 7.1, respectively. RNA interference-mediated silencing of *Foxq1*, *Foxf1a*, and *Foxb1*, but not *Foxd4*, *Foxg1*, *and Foxf2* led to ES49 cell growth inhibition (Figure 2C). Expression of *FOXQ1*, *FOXF1*, and *FOXB1* was then examined in a series of human sarcomas. High levels of *FOXQ1* expression in human Ewing sarcoma were also observed by GEO database search using a series of human sarcoma microarray analyses (37 cases of Ewing sarcoma, 6 alveolar soft part sarcoma, 21 osteosarcoma, 57 rhabdomyosarcoma, and 34 synovial sarcoma) (Figure 2D). *FOXQ1* expression was detected in the human Ewing sarcoma cell lines KH and EWS, whereas no *FOXF1* and *FOXB1* expression was observed in these cell lines (Figure 2E). Knockdown of *FOXQ1* suppressed EWS cell growth (Figure 2F), suggesting that FOXQ1 plays an important role in EWS-FLI1–mediated gene regulation and Ewing sarcoma maintenance and/or progression.

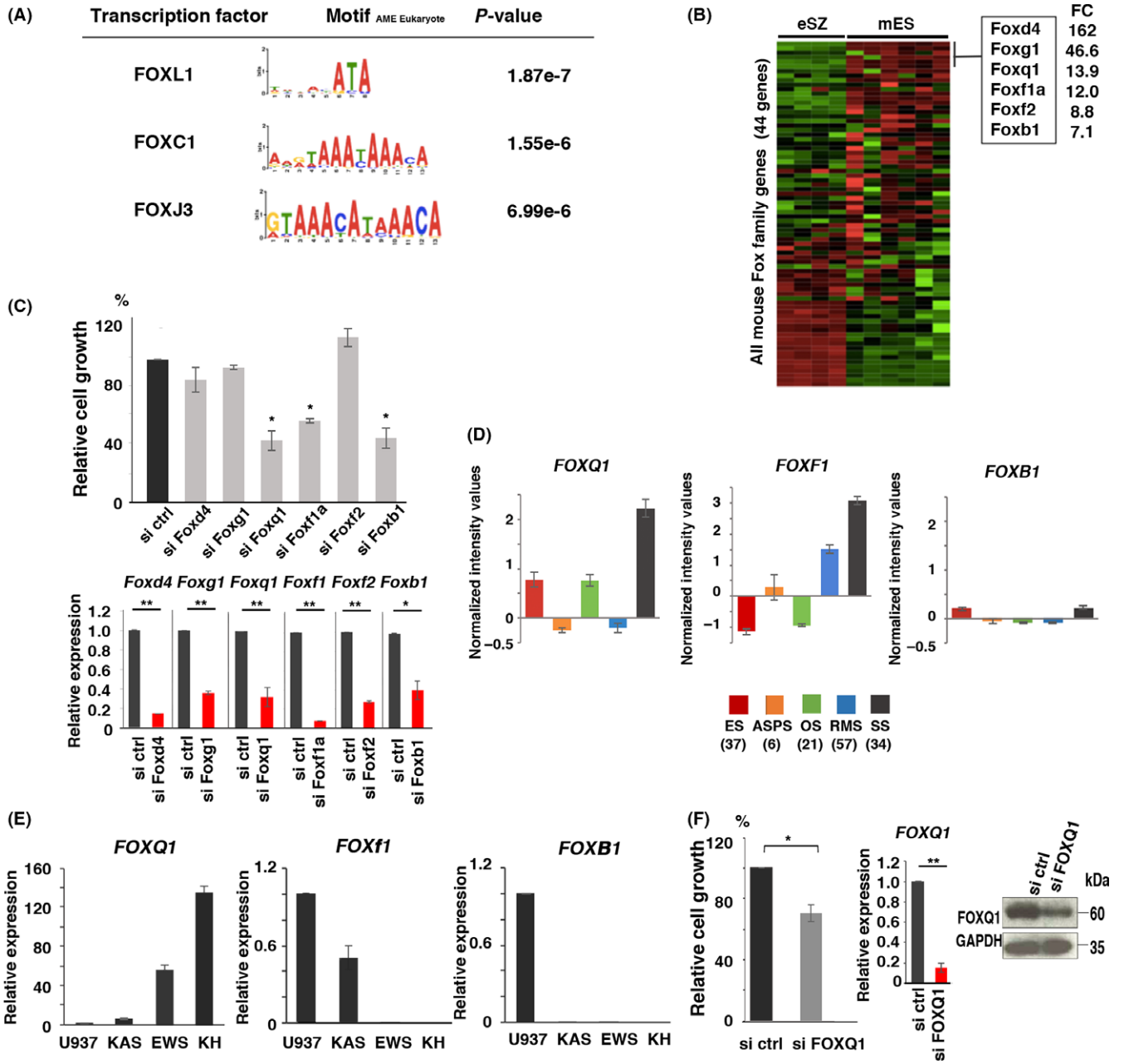

FIGURE 2 Detection of FOX binding motifs and upregulation of Foxq1 in Ewing sarcoma. A, AME suite motif analysis identification of enrichment of FOX binding motifs within EWS-FLI1-binding peaks. B, Heatmap of expression for 44 murine Fox family genes in mouse Ewing sarcoma (mES) and embryonic superficial zone (eSZ).[5] Six Fox family genes are highlighted in the box with fold changes of expression compared to eSZ. C, Growth suppression of ES49 cells by siRNA-mediated gene silencing (top). Data represent the means ± SEM of 3 independent experiments (*$P < .01$). Efficiencies of gene silencing were assessed as relative gene expression to *Gapdh* mRNA by real-time qPCR (bottom). Data represent the means ± SEM of 3 independent experiments (*$P < .02$, **$P < .001$). D, Expression of *FOXQ1*, *FOXF1*, and *FOXB1* in human sarcoma. Gene expression levels were compared on microarray data obtained from the Gene Expression Omnibus (GEO) database. ES, Ewing sarcoma; ASPS, alveolar soft part sarcoma; OS, osteosarcoma; RMS, rhabdomyosarcoma; SS, synovial sarcoma. Numbers of each sarcoma case examined are indicated. E, Expression of *FOXQ1*, *FOXF1*, and *FOXB1* in human sarcoma cell lines. U937, monocytic leukemia; KAS, clear cell sarcoma; EWS, Ewing sarcoma with EWS-FLI1; KH, Ewing sarcoma with EWS-ERG. Normalized gene expression levels to *GAPDH* mRNA are indicated as the average of normalized intensity values obtained by real-time qPCR. F, Growth suppression of EWS human Ewing sarcoma cells by *FOXQ1* silencing (left). Efficiency of gene silencing was assessed as relative gene expression to *Gapdh* mRNA by real-time qPCR (center). Data represent the means ± SEM of 3 independent experiments (*$P < .02$, **$P < .001$). Efficiency of *FOXQ1* silencing was confirmed by western blotting (right)

3.3 | EWS-FLI1 and Foxq1 co-regulate the transcriptional machinery

The genes containing EWS-FLI1-binding peaks that include both GGAA microsatellites and FoBS were further investigated. Within these binding regions, 20 out of 26 sites/genes contained FoBS within 100 bp from GGAA microsatellites (Table 2). Considering their cancer-associated functions, we focused subsequent investigations on *Trib1* and *Nrg1*. *Trib1* was identified as a leukemia disease gene that enhances MAPK phosphorylation and degrades C/EBPα.[22-24] *Nrg1* promotes tumor progression in many cancers such as gastric, lung, and breast cancers.[25–27] Notably, these genes have been previously identified as EWS-FLI1-binding genes in human Ewing sarcoma.[4] EWS-FLI1-binding peaks and an H3K27Ac active enhancer mark could be observed 30 kbp upstream from the TSS of *Trib1* and 164 kbp downstream from that of *Nrg1* (Figure 3A). In particular, the EWS-FLI1-binding peak at the *Trib1* locus was located within the super-enhancer site (Figure 1E). Enhancer activities of these regions were then examined using luciferase reporter vectors with the sequences that encompass both GGAA microsatellites and FoBS. High enhancer activities were observed when *Trib1* or *Nrg1* reporter constructs were transfected into human U2OS osteosarcoma cells in the presence of EWS-FLI1 (Figure 3B). Whereas Foxq1 alone exhibited few enhancing effects, co-transfection of EWS-FLI1 and Foxq1 significantly increased the enhancer activity ($P < .001$) (Figure 3B), suggesting that Foxq1 promotes transactivation of target genes regulated by EWS-FLI1. In addition, knockdown of *Foxq1* or *EWS-FLI1* suppressed both *Trib1* and *Nrg1* expression in ES49 and EWS cells (Figure 3C). Although no synergistic effect was observed between Foxq1 and EWS-FLI1 silencing, their cooperation might be critical for *Trib1* and *Nrg1* regulation.

3.4 | Foxq1 interacts with EWS-FLI1 through the N-terminus of EWS

Interaction between Foxq1 and EWS-FLI1 was examined using co-immunoprecipitation assay. ES49 cells were transfected with an HA-tagged *Foxq1* expression plasmid, immunoprecipitated with an anti-HA antibody, and EWS-FLI1 was detected by western blotting (Figure 4A). Reciprocal immunoprecipitations in EWS-FLI1–overexpressing and Foxq1-overexpressing 239T cells were carried out to determine whether Foxq1 interacts with the EWS or FLI1 sites of EWS-FLI1. Cells were immunoprecipitated with anti-HA or anti-FLAG antibodies followed by western blotting. As shown in Figure 4B, Foxq1 interacts with EWS-FLI1 and EWS but not with FLI1, indicating that the cooperative action of Foxq1 is only effective for EWS-FLI1 fusion but not for wild-type FLI1.

3.5 | Trib1 and Nrg1 promote Ewing sarcoma cell growth

To clarify the role of Trib1 and Nrg1 in Ewing sarcoma proliferation and survival, RNA interference-mediated gene silencing experiments were carried out. Knockdown of *Trib1* or *Nrg1* suppressed proliferation of ES49 cells (Figure 5A). Efficiencies of growth inhibition by *Trib1* or *Nrg1* knockdown were less than that by *FLI1* knockdown but equivalent to that by *Foxq1* knockdown. Notably, no synergistic effect of growth suppression between *Trib1* and *Nrg1* knockdown was observed, suggesting that these genes might function in the overlapping pathways. Similar results were obtained in human EWS cells (Figure 5B). No apparent morphological alterations were observed in human and mouse Ewing sarcoma cells by *Trib1* or *Nrg1* silencing (data not shown). Furthermore, EdU incorporation was reduced by Trib1 knockdown, whereas no increase of Annexin V-positive pre-apoptotic cells was found (Figure 5C,D). As Trib1 induces the degradation of C/EBP proteins by recruiting the ubiquitin E3 ligase COP1,[24,28] protein expression of C/EBPα and β was next examined. Although C/EBPα is not expressed in Ewing sarcoma cells (data not shown), the LAP isoform of C/EBPβ were increased by *Trib1* silencing (Figure 5E). Increased expression levels of *TRIB1* and *NRG1* were also observed in human Ewing sarcoma samples compared to those in other sarcoma types (Figure 5F). Exogenous overexpression of Trib1 or Nrg1 did not enhance sarcoma cell growth (Figure S1). Perhaps, upregulation of these genes by EWS-FLI1 and Foxq1 is sufficient for proliferation of Ewing sarcoma cells. Collectively, these data indicate that *Trib1* and *Nrg1* comprise important target genes of EWS-FLI1 as well as FOXQ1 for promoting cell cycle progression and cellular survival in Ewing sarcoma.

4 | DISCUSSION

In the present study, we identified global DNA binding of EWS-FLI1 in mouse Ewing sarcoma. Our previous study indicated that the gene expression profiles are very similar between human and mouse Ewing sarcoma,[5] suggesting that a common gene regulatory function of EWS-FLI1 is present in both organisms. In addition, GGAA microsatellites were also detected as EWS-FLI1–specific binding sites in mouse Ewing sarcoma, although the frequency was lower than that in human Ewing sarcoma. Furthermore, histone H3K27Ac was frequently associated with GGAA microsatellites showing EWS-FLI1 binding, suggesting that such binding was involved in chromatin remodeling. However, the genomic distribution of GGAA microsatellites is not conserved between human and mouse, and the nearest genes from EWS-FLI1-bound microsatellites differed markedly between the 2 species. As gene regulation is modulated by super-enhancers with impact over long distances,[29] this mechanism as well as the higher order topology of chromatin should be considered with regard to understanding EWS-FLI1 function in Ewing sarcoma.

We have compared EWS-FLI1-binding data of our ChIP-Seq analysis with that of EWS-FLI1–induced murine osteosarcoma.[30] Ninety-nine of 246 (40%) EWS-FLI1-binding peaks in our study were also detected in osteosarcoma samples, despite the phenotypic differences between Ewing sarcoma and osteosarcoma (Doc. S5). In contrast, EWS-FLI1 binding on GGAA microsatellites in murine

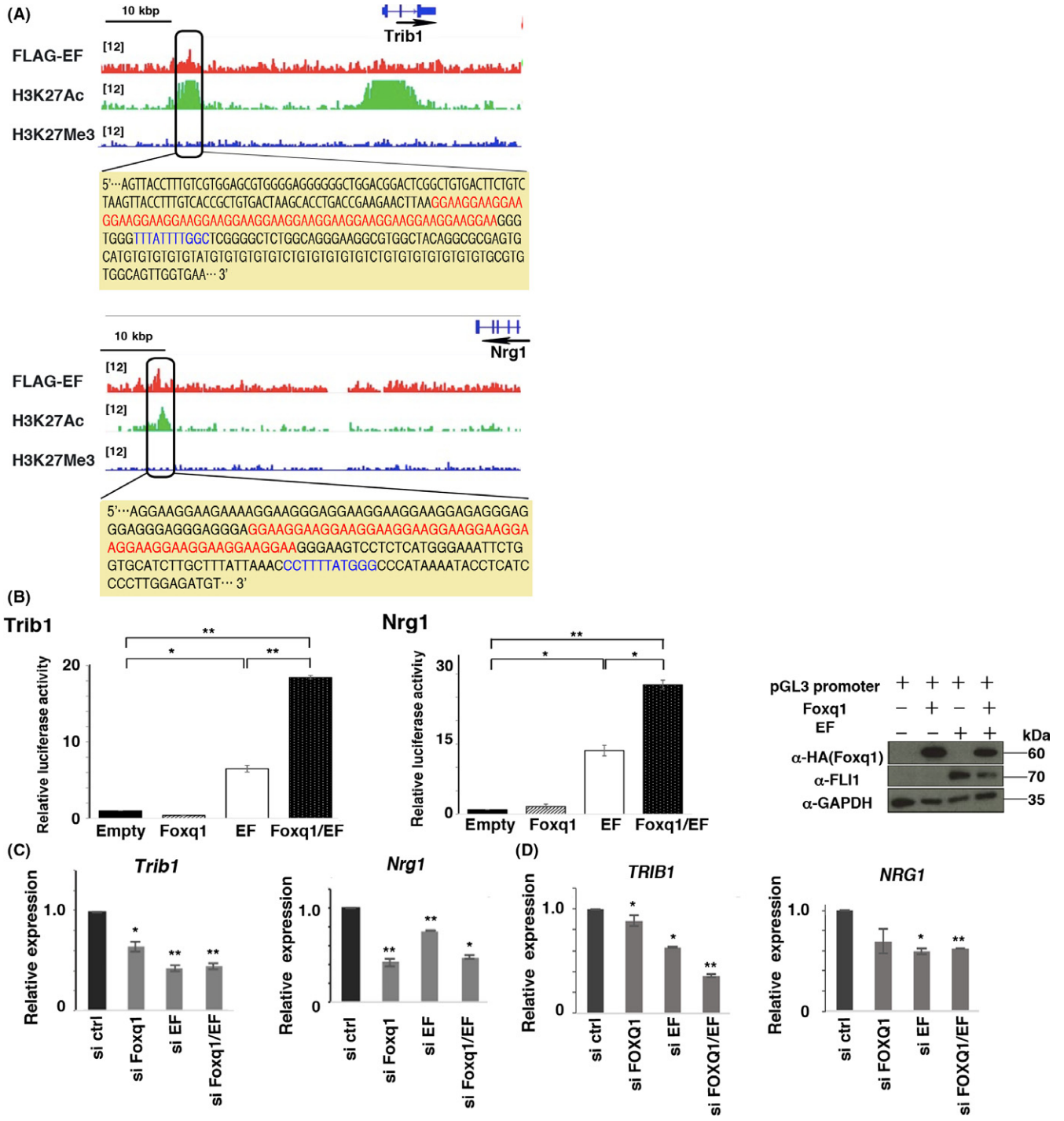

FIGURE 3 EWS-FLI1 and Foxq1 coregulate target genes. A, EWS-FLI1 binding peaks at *Trib1* (top) and *Nrg1* (bottom) loci. Sequences around the peaks are shown in yellow boxes and GGAA microsatellites and FOX binding motifs are indicated in red or blue, respectively. Arrows indicate transcription orientation of each gene. B, Luciferase reporter assay. The DNA fragments indicated in (A) were introduced into the pGL3 promoter vector. Relative luciferase activities are shown in the presence or absence of Foxq1 and/or EWS-FLI1 (EF) (left and center). Data represent the means ± SEM of 3 independent experiments (*$P < .002$, **$P < .001$). Protein expression of Foxq1 and EWS-FLI1 is shown (right). C, Effect of *Foxq1* or *EWS-FLI1* silencing on *Trib1* and *Nrg1* expression in mouse Ewing sarcoma as detected by real-time qPCR. Expression levels were normalized to *Gapdh* mRNA. Data represent the means ± SEM of 3 independent experiments (*$P < .002$, **$P < .001$). D, Effect of *FOXQ1* or *EWS-FLI1* silencing on *TRIB1* and *NRG1* in human Ewing sarcoma as detected by real-time qPCR. Expression levels were normalized to *GAPDH* mRNA. Data represent the means ± SEM of 3 independent experiments (*$P < .05$, **$P < .01$)

osteosarcoma was also significantly different from that in human Ewing sarcoma, indicating that there is species-specific DNA binding for EWS-FLI1.

Sequence analysis of EWS-FLI1-binding peaks suggested possible cooperative binding with FOX family transcription factors. There are 44 members of the FOX family genes in human and mouse.[31] Gene

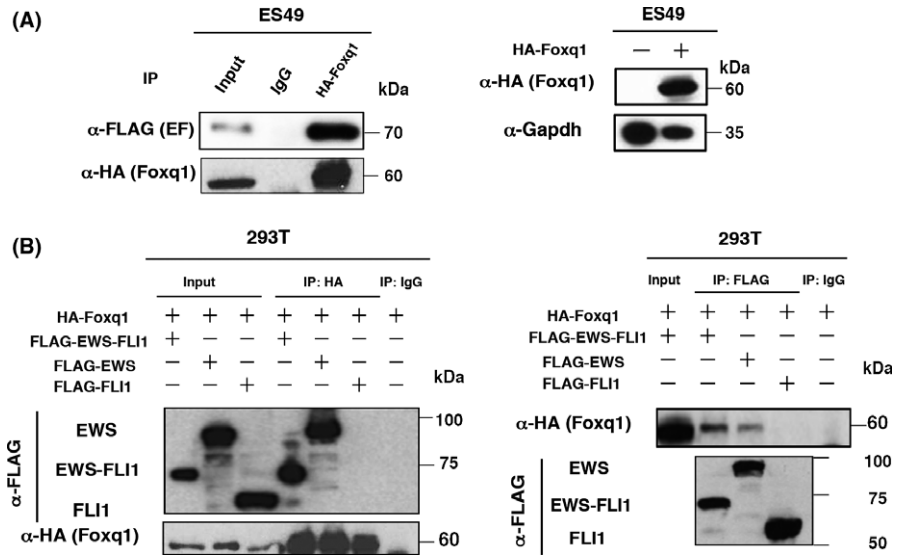

FIGURE 4 EWS-FLI1 interacts with Foxq1 through its EWS region. A, ES49 cells were transiently transfected with HA-tagged Foxq1. Cell lysates were immunoprecipitated with an anti-HA monoclonal antibody and immunoblotted with rabbit polyclonal anti-FLAG or anti-HA antibodies (left). Expression of HA-tagged Foxq1 was assessed by immunoblotting whole cell lysates with an anti-HA antibody. Gapdh serves as loading control (right). B, 293T cells were transiently transfected with HA-tagged Foxq1 and HA-tagged EWS-FLI1, EWS or FLI1. The cell lysates were immunoprecipitated with mouse monoclonal anti-HA (left) or anti-FLAG (right) antibodies and immunoblotted with indicated antibodies

expression and functional analysis identified FOXQ1 as the FOX protein responsible for serving as a co-binding partner of EWS-FLI1. FOXQ1 is involved in a series of human cancers and it affects several important signaling networks. Specifically, FOXQ1 is overexpressed in colorectal cancer and it promotes tumor growth and/or metastatic activity by increasing PI3K/AKT signaling.[32,33] EMT, which is related to tumor stemness and chemoresistance, is promoted by FOXQ1 in nonsmall cell lung cancer and breast cancer.[34,35] Notably, the expression of EMT markers and upregulation of PI3K signals in Ewing sarcoma are associated with worse prognosis.[36] Our current study indicates that FOXQ1 interacts with EWS-FLI1 and increases its enhancer activity toward target genes. However, the present results did not exclude the possible involvement of other Fox family genes in Ewing sarcoma, given the potential limitations of gene silencing validation as a result of a lack of suitable antibodies for several Fox proteins.

Trib1 and *Nrg1* are identified as target genes regulated by EWS-FLI1 and FOXQ1. EWS-FLI1 peaks were detected in the vicinity of *TRIB1* and *NRG1* in human Ewing sarcoma,[4] and gene silencing of these genes suppressed cell growth of both mouse and human Ewing sarcoma cells. *TRIB1* acts as an oncogene with strong transforming activity in acute myelogenous leukemia,[22,23,37] and Tribbles family genes are also involved in human solid cancers.[38] It is therefore notable that *Trib1* knockdown suppressed Ewing sarcoma cell growth concomitant with increased levels of C/EBPβ. A recent study suggested that overexpression of C/EBPβ increased the transformation activity of Ewing sarcoma cells, although it did not affect cell proliferation or viability,[39] suggesting that a complex feedback loop may exist in C/EBPβ regulation. *Nrg1* encodes neuregulin 1 or heregulin, the predominant ligand for ERBB3, and NRG1/ERBB signals are important in cellular development such as for Schwann cells and the cardiovascular system.[40–42] This signaling axis is also important in multiple cancer types and activation of the signal promotes cancer cell migration or drug resistance.[27,43,44] Although the exact functions of TRIB1 and NRG1 in clinical cases of Ewing sarcoma remain to be clarified, the present study highlighted their potential roles as therapeutic targets and/or biomarkers.

There are significant differences in Ewing sarcoma susceptibility among human races.[45] Copy number variation of GGAA microsatellites has been reported and the variation at the EGR2 locus in Ewing sarcoma development was found to be associated with increased gene expression.[46] Distribution and copy numbers of GGAA microsatellites in mice completely differ from those in humans. Nevertheless, the morphological and biological phenotypes of the mouse Ewing sarcoma model recapitulate those of the human tumors. The significance of the GGAA microsatellite-mediated EWS-FLI1 function and our understanding of target gene regulation should therefore be carefully reconsidered. Alternatively, oncogenic activity by EWS-FLI1 may be afforded by its global binding to GGAA microsatellites to impact dynamic chromatin remodeling.

In conclusion, our study showed the relationship between EWS-FLI1 and GGAA microsatellites, identified Foxq1 as a novel interaction partner of EWS-FLI1, and highlighted *Trib1* and *Nrg1* as important downstream target genes of the interaction. These findings will likely be of importance for further understanding the oncogenic role of EWS-FLI1 and the mechanisms of Ewing sarcoma development.

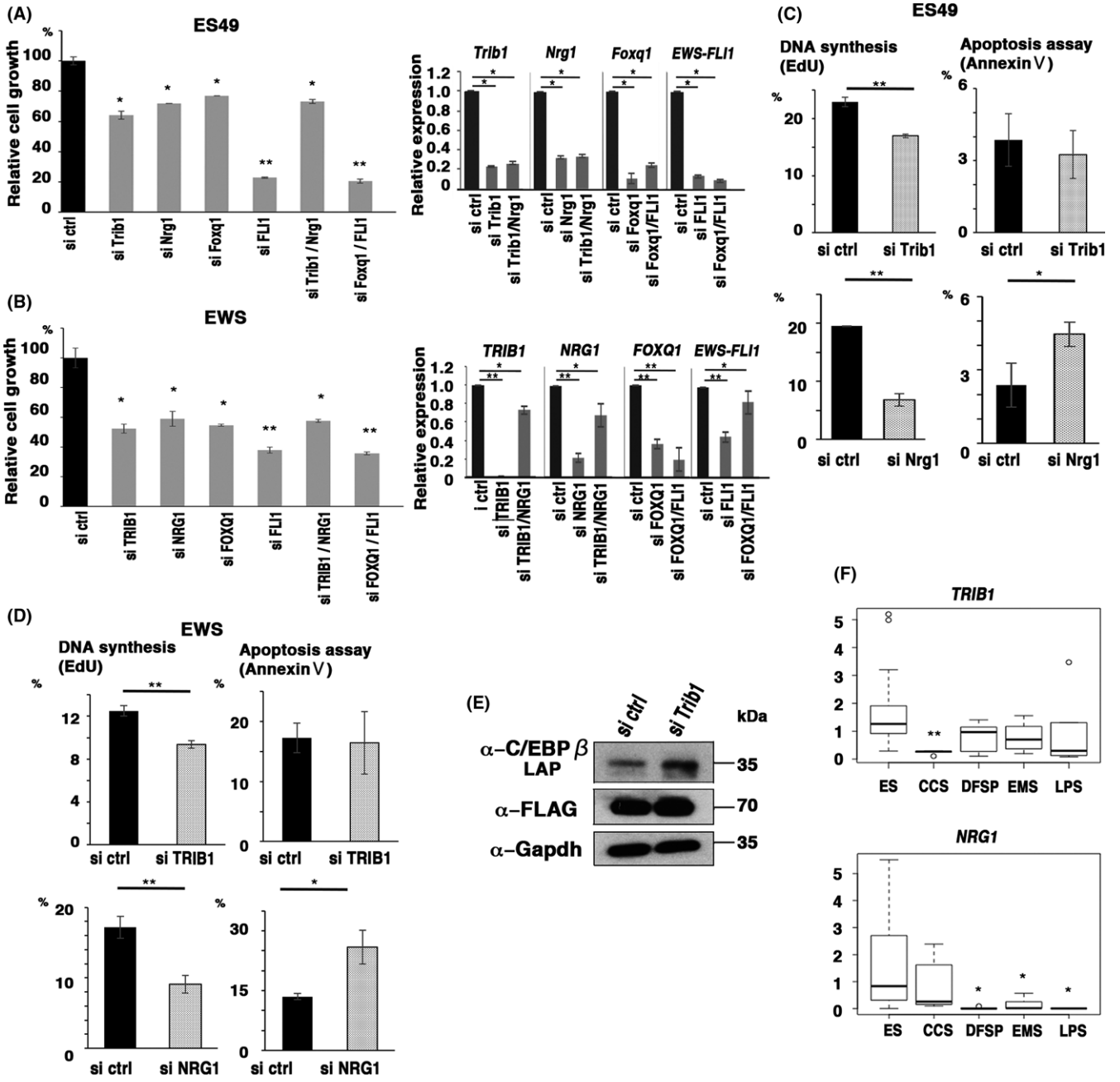

FIGURE 5 *Trib1* and *Nrg1* are involved in Ewing sarcoma proliferation and survival. A, Growth inhibition of ES49 cells by gene silencing (left). Cell numbers were counted 48 h after transfection of siRNAs. Relative cell growth compared with control siRNA infection is indicated. Data represent the means ± SEM of 3 independent experiments (*$P < .02$, **$P < .01$). Efficiencies of gene silencing was assessed as relative gene expression to *Gapdh* mRNA by real-time qPCR (right). Data represent the means ± SEM of 3 independent experiments (*$P < .001$). B, Growth inhibition of EWS human Ewing sarcoma cells by gene silencing (left). Cell numbers were counted 48 h after transfection of siRNAs. Relative cell growth compared with control siRNA infection is indicated. Data represent the means ± SEM of 3 independent experiments (*$P < .01$, **$P < .001$). Efficiencies of gene silencing were assessed as relative gene expression to *GAPDH* mRNA by real-time qPCR (right). Data represent the means ± SEM of 3 independent experiments (*$P < .05$, **$P < .001$). C, Effects of *Trib1* or *Nrg1* knockdown on DNA synthesis or apoptosis in ES49 cells. DNA synthesis and apoptosis were quantitated by measuring frequencies of EdU- or Annexin V-positive cells by FACS, respectively. Data represent the means ± SEM of 3 independent experiments (*$P < .05$, **$P < .01$). D, Effects of *TRIB1* or *NRG1* knockdown on DNA synthesis or apoptosis in EWS cells. DNA synthesis and apoptosis were quantitated by measuring frequencies of EdU- or Annexin V-positive cells by FACS, respectively. Data represent the means ± SEM of 3 independent experiments (*$P < .05$, **$P < .01$). E, Immunoblotting shows expression of C/EBPβ in ES49 cells upon *Trib1* knockdown. The LAP isoform of C/EBPβ is indicated. F, TRIB1 and NRG1 expression in human sarcoma samples assessed by real-time qPCR. ES, Ewing sarcoma; CCS, clear cell sarcoma; DFSP, dermatofibrosarcoma protuberans; EMS, extraskeletal myxoid chondrosarcoma; LPS, liposarcoma

ACKNOWLEDGMENTS

We thank T Yokoyama for assisting with the ChIP-Seq analysis. This work was supported by a Grant-in-Aid for Scientific Research from Japan Society for the Promotion of Science (26250029 to T.N. and 16K07131 to M.T.), and by a Research Grant from the Mitsubishi Foundation (29133 to T.N.).

CONFLICTS OF INTEREST

T. Nakamura reports receiving a commercial research grant from Otsuka Pharmaceutical Co. Ltd. No potential conflicts of interest were disclosed by the other authors.

ORCID

Takuro Nakamura http://orcid.org/0000-0002-0419-7547

REFERENCES

1. Gaspar N, Hawkins DS, Dirksen U, et al. Ewing sarcoma: current management and future approaches through collaboration. *J Clin Oncol*. 2015;33:3036-3046.
2. Delattre O, Zucman J, Plougastel B, et al. Gene fusion with an ETS DNA-binding domain caused by chromosome translocation in human tumours. *Nature*. 1992;359:162-165.
3. Riggi N, Suva ML, Suva D, et al. EWS-FLI-1 expression triggers a Ewing's sarcoma initiation program in primary human mesenchymal stem cells. *Cancer Res*. 2008;68:2176-2185.
4. Riggi N, Knoechel B, Gillespie SM, et al. EWS-FLI1 utilizes divergent chromatin remodeling mechanisms to directly activate or repress enhancer elements in Ewing sarcoma. *Cancer Cell*. 2014;28:668-681.
5. Tanaka M, Yamazaki Y, Kanno Y, et al. Ewing's sarcoma precursors are highly enriched in embryonic osteochondrogenic progenitors. *J Clin Invest*. 2014;124:3061-3074.
6. Tanaka M, Yamaguchi M, Yamazaki Y, et al. Somatic chromosomal translocation between Ewsr1 and Fli1 loci leads to dilated cardiomyopathy in a mouse model. *Sci Rep*. 2015;5:7826.
7. Minas TZ, Surdez D, Javaheri T, et al. Combined experience of six independent laboratories attempting to create an Ewing sarcoma mouse model. *Oncotarget*. 2017;8:34141-34163.
8. Boulay G, Sandoval GJ, Riggi N, et al. Cancer-specific retargeting of BAF complexes by a prion-like domain. *Cell*. 2017;171:163-178.
9. Brohl AS, Solomon DA, Chang W, et al. The genomic landscape of the Ewing sarcoma family of tumors reveals recurrent STAG2 mutation. *PLoS Genet*. 2014;10:e1004475.
10. Crompton BD, Stewart C, Taylor-Weiner A, et al. The genomic landscape of pediatric Ewing sarcoma. *Cancer Discov*. 2014;4:1326-13451.
11. Tirode F, Surdez D, Ma X, et al. Genomic landscape of Ewing sarcoma defines an aggressive subtype with co-association of STAG2 and TP53 mutations. *Cancer Discov*. 2014;4:1342-1353.
12. Gangwal K, Sankar S, Hollenhorst PC, et al. Microsatellites as EWS/FLI1 response elements in Ewing's sarcoma. *Proc Natl Acad Sci USA*. 2008;105:10149-10154.
13. Guillon N, Tirode F, Boeva V, Zynovyev A, Barillot E, Delattre O. The oncogenic EWS-FLI1 protein binds in vivo GGAA microsatellite sequences with potential transcriptional activation function. *PLoS One*. 2009;4:e4932.
14. Yokoyama T, Nakatake M, Kuwata T, et al. MEIS1-mediated transactivation of synaptotagmin like 1 promotes CXCL12/CXCR4 signaling and leukemogenesis. *J Clin Invest*. 2016;126:1664-1678.
15. Whyte WA, Orlando DA, Hnisz D, et al. Master transcription factors and mediator establish super-enhancers at key cell identity genes. *Cell*. 2013;153:307-319.
16. Loven J, Hoke HA, Lin CY, et al. Selective inhibition of tumor oncogenes by disruption of super-enhancers. *Cell*. 2013;153:320-334.
17. Yoshimoto T, Tanaka M, Homme M, et al. CIC-DUX4 induces small round cell sarcomas distinct from Ewing sarcoma. *Cancer Res*. 2017;77:2927-2937.
18. Tomazou EM, Sheffield NC, Schmidl C, et al. Epigenome mapping reveals distinct modes of gene regulation and widespread enhancer reprogramming by the oncogenic fusion protein EWS-FLI1. *Cell Rep*. 2015;10:1082-1095.
19. Tanaka M, Homme M, Yamazaki Y, Shimizu R, Takazawa Y, Nakamura T. Modeling alveolar soft part sarcoma unveils novel mechanisms of metastasis. *Cancer Res*. 2017;77:897-907.
20. Ordóñez JL, Osuna D, Herrero D, de Alava E, Madoz-Gúrpide J. Advances in Ewing's sarcoma research: where are we now and what lies ahead? *Cancer Res*. 2009;69:7140-7150.
21. Cidre-Aranaz F, Alonso J. EWS/FLI1 target genes and therapeutic opportunities in Ewing sarcoma. *Front Oncol*. 2015;5:162.
22. Jin G, Yamazaki Y, Takuwa M, et al. Trib1 and Evi1 cooperate with Hoxa and Meis1 in myeloid leukemogenesis. *Blood*. 2007;109:3998-4005.
23. Yokoyama T, Kanno Y, Yamazaki Y, Takahara T, Miyata S, Nakamura T. Trib1 links the MEK1/ERK pathway in myeloid leukemogenesis. *Blood*. 2010;116:2768-2775.
24. Yokoyama T, Nakamura T. Trib1 in disease; signaling pathways important for cellular function and neoplastic transformation. *Cancer Sci*. 2011;102:1115-1122.
25. Dhanasekaran SM, Balbin OA, Chen G, et al. Transcriptome meta-analysis of lung cancer reveals recurrent aberrations in NRG1 and Hippo pathway genes. *Nat Commun*. 2014;5:5893.
26. Han ME, Kim HJ, Shin DH, Hwang SH, Kang CD, Oh SO. Overexpression of NRG1 promotes progression of gastric cancer by regulating the self-renewal of cancer stem cells. *J Gastroenterol*. 2015;50:645-656.
27. Leung W, Roxanis I, Sheldon H, et al. Combining lapatinib and pertuzumab to overcome lapatinib resistance due to NRG1-mediated signalling in HER2-amplified breast cancer. *Oncotarget*. 2015;6:5678-5694.
28. Yoshida A, Kato JY, Nakamae I, Yoneda-Kato N. COP1 targets C/EBPa for degradation and induces acute myeloid leukemia via Trib1. *Blood*. 2013;122:1750-1760.
29. Tang Z, Luo OJ, Li X, et al. CTCF-mediated human 3D genome architecture reveals chromatin topology for transcription. *Cell*. 2015;163:1611-1627.
30. Komura S, Semi K, Itakura F, et al. An EWS-FLI1-induced osteosarcoma model unveiled a crucial role of impaired osteogenic differentiation on osteosarcoma development. *Stem Cell Rep*. 2016;6:592-606.
31. Golson ML, Kaestner KH. Fox transcription factors: from development to disease. *Development*. 2016;143:4558-4570.
32. Kaneda H, Arao T, Tanaka K, et al. FOXQ1 is overexpressed in colorectal cancer and enhances tumorigenicity and tumor growth. *Cancer Res*. 2010;70:2053-2063.
33. Liu JY, Wu XY, Wu GN, Liu FK, Yao XQ. FOXQ1 promotes cancer metastasis by PI3K/AKT signaling regulation in colorectal carcinoma. *Am J Transl Res*. 2017;9:2207-2218.
34. Feng J, Xu L, Ni S, et al. Involvement of FoxQ1 in NSCLC through regulating EMT and increasing chemosensitivity. *Oncotarget*. 2014;5:9689-9702.

35. Meng F, Speyer CL, Zhang B, et al. PDGFRα and β play critical roles in mediating Foxq1-driven breast cancer stemness and chemoresistance. *Cancer Res*. 2015;75:584-593.
36. Machado I, López-Guerrero JA, Navarro S, et al. Epithelial cell adhesion molecules and epithelial mesenchymal transition (EMT) markers in Ewing's family of tumors (ESFTs). Do they offer any prognostic significance? *Virchows Arch*. 2012;461:333-337.
37. Yokoyama T, Toki T, Aoki Y, et al. Identification of TRIB1 R107L gain-of-function mutation in human acute megakaryocytic leukemia. *Blood*. 2012;119:2608-2611.
38. Eyers PA, Keeshan K, Kannan N. Tribbles in the 21st century: The evolving roles of Tribbles pseudokinases in biology and disease. *Trends Cell Biol*. 2017;27:284-298.
39. Gardiner JD, Abegglen LM, Huang X, et al. C/EBPβ-1 promotes transformation and chemoresistance in Ewing sarcoma cells. *Oncotarget*. 2017;8:26013-26026.
40. Holmes WE, Sliwkowski MX, Akita RW, et al. Identification of heregulin, a specific activator of p185erbB2. *Science*. 1992;256:1205-1210.
41. Newbern J, Birchmeier C. Nrg1/ErbB signaling networks in Schwann cell development and myelination. *Semin Cell Dev Biol*. 2010;21:922-928.
42. Odiete O, Hill MF, Sawyer DB. Neuregulin in cardiovascular development and disease. *Circ Res*. 2012;111:1376-1385.
43. Haskins JW, Nguyen DX, Stern DF. Neuregulin 1-activated ERBB4 interacts with YAP to induce Hippo pathway target genes and promote cell migration. *Sci Signal*. 2014;7:ra116.
44. Cheng H, Terai M, Kageyama K, et al. Paracrine effect of NRG1 and HGF drives resistance to MEK inhibitors in metastatic uveal melanoma. *Cancer Res*. 2015;75:2737-2748.
45. Jawad MU, Cheung MC, Min ES, Schneiderbauer MM, Koniaris LG, Scully SP. Ewing sarcoma demonstrates racial disparities in incidence-related and sex-related differences in outcome: an analysis of 1631 cases from the SEER database, 1973-2005. *Cancer*. 2009;115:3526-3536.
46. Grünewald TG, Bernard V, Gilardi-Hebenstreit P, et al. Chimeric EWSR1-FLI1 regulates the Ewing sarcoma susceptibility gene EGR2 via a GGAA microsatellite. *Nat Genet*. 2015;47:1073-1078.

SUPPORTING INFORMATION

Additional supporting information may be found online in the Supporting Information section at the end of the article.

How to cite this article: Shimizu R, Tanaka M, Tsutsumi S, et al. EWS-FLI1 regulates a transcriptional program in cooperation with Foxq1 in mouse Ewing sarcoma. *Cancer Sci*. 2018;109:2907–2918. https://doi.org/10.1111/cas.13710